

Inclusive and exclusive diffraction: overview of the experimental presentations at Diffraction2004

Aharon Levy^a *

^a Raymond and Beverly Sackler Faculty of Exact Sciences, School of Physics and Astronomy, Tel Aviv University, Tel Aviv, Israel

Some issues in inclusive and exclusive diffractive processes are discussed.

1. Introduction

There were 20 experimental presentations at this conference, all by expert people in the field. All these talks were plenary, so there is no point of me summarizing again the contents of each talk. Instead, I would like to present a personal view and touch upon few selected issues which were presented here.

2. What is diffraction?

In spite of the fact that diffractive processes have a long history, it is still not easy to give a precise and concise definition of what one calls a diffractive reaction. It is clearly a process where, in an exchange picture, no color is exchanged. This however includes all the colorless particles. A further requirement is that the exchanged messenger has the quantum number of the vacuum, which, in the Regge picture is named the Pomeron. Elastic scattering is usually presented as an example of a diffractive process. However, at low energies it can proceed also through an exchange with quantum numbers different from the vacuum, called a Reggeon. At high energies, where the kinematics allows for a large rapidity range, it is more useful to talk about rapidity gaps. Due to the fact that no color is exchanged, there is a suppression of gluon radiation and therefore a rapidity gap is produced between the two vertices of the interaction. Of course, both the Pomeron and the Reggeon are

colorless, however the rapidity gap produced by a Reggeon is exponentially suppressed, while that of the Pomeron remains constant. This prompted Bjorken [1] to define diffraction as processes in which the large rapidity gap is not exponentially suppressed.

How practical is this definition? This we shall see in the following sections.

3. Diffraction in inclusive processes

3.1. Kinematical variables

I will try to define here all the variables needed in the following sections. Let us first look at a diffractive reaction $ep \rightarrow epX$ at HERA, depicted in figure 1. A virtual photon γ^* ($Q^2 \equiv -q^2$) in-

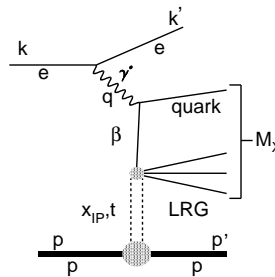


Figure 1. Schematic representation of the deep inelastic diffractive scattering.

interacts with the proton through a colorless ex-

*Supported in part by the Israel Science Foundation (ISF).

change with vacuum quantum numbers. A mass M_X of the hadronic system recoils against the proton. The square of the momentum transfer at the proton vertex is t . The fraction of the proton momentum carried by the exchange is denoted by x_P . The quark struck by the virtual photon carries a fraction β of the momentum of the colorless exchange. (Note that sometimes z is used instead of β). The last two variables are connected to Bjorken x as follows: $x = \beta x_P$.

At the Tevatron, where one studies the diffractive reaction $\bar{p}p \rightarrow \bar{p}X$, the equivalent variable to x_P is denoted by ξ .

3.2. Selecting diffractive processes

There are three methods used at HERA to select diffractive events. One [2] uses the Leading Proton Spectrometer (LPS) to detect the scattered proton and by choosing the kinematic region where the scattered proton loses very little of its initial longitudinal energy, it ensures that the event was diffractive. A second method [3] simply request a large rapidity gap (LRG) in the event and fits the data to contributions coming from Pomeron and Reggeon exchange. The third method [4] uses the distribution of the mass of the hadronic system seen in the detector, M_X , to isolate diffractive events. We will refer to these three as LPS, LRG and M_X methods. At the Fermilab Tevatron [5] diffractive processes are being studied by tagging events with either a rapidity gap or a leading hadron.

The LPS method has the advantage of detecting the scattered proton and thus excluding proton dissociative processes. However, in order to ensure that the scattered proton resulted from a diffractive process, one requires $x_P < 0.01$, where x_P is the amount of longitudinal momentum lost by the scattered proton. This cut removes contributions coming from Reggeon exchanges [6].

The LRG method selects events which also include some proton dissociative processes and Reggeon contributions. The latter can be removed by the same $x_P < 0.01$ cut as above. The proton dissociative processes can be removed provided their mass is large enough to produce signals in some forward tagging devices. The contribution of low mass proton dissociation can be es-

timated. In the analysis of the H1 collaboration, processes with proton dissociation into masses below 1.6 GeV amount to about 10% [7].

The M_X method which subtracts the exponentially suppressed large rapidity gap events, in principle subtracts also the Reggeon contribution and is left only with the proton dissociative background. These can not be removed for masses below 2.4 GeV, which constitutes about 30% of the selected diffractive events [8].

At the Tevatron, single diffractive events, $\bar{p}p \rightarrow \bar{p}X$, are selected by tagging the scattered \bar{p} .

3.3. Diffractive structure function

In figure 2 the diffractive structure function measurements with all three HERA methods are presented. The M_X data have been multiplied by a factor of 0.69 to correct for the proton dissociation background. No correction was done to the H1 data. All methods seem in general to agree with each other in their overlapping kinematic region.

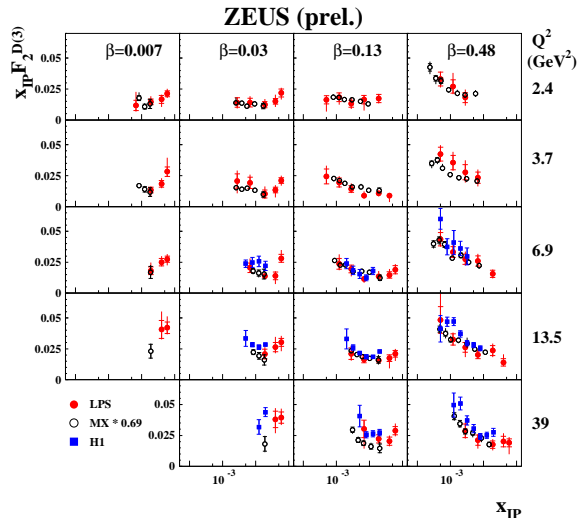


Figure 2. Comparison of $x_P F_2^{D(3)}$ measured by H1 and ZEUS, as a function of x_P in overlapping bins of β and Q^2 .

3.4. Q^2 dependence of λ

The x behaviour of the inclusive structure function F_2 at a given Q^2 is well described by an $x^{-\lambda}$ form. The value of λ is connected to the Pomeron intercept, $\lambda = \alpha_P(0) - 1$. The value of λ is approximately constant till $Q^2 \approx 1 \text{ GeV}^2$, and then rises almost linearly with $\ln Q^2$.

It is of interest to see whether the x_P behaviour of $x_P F_2^{D(3)}$ shows a similar pattern. To this end, a fit of the form $x_P F_2^{D(3)} \propto x_P^{-\lambda}$ was performed, for different Q^2 intervals.

Figure 3 shows the value of λ as function of Q^2 from fits to the x behaviour of F_2 and from the x_P behaviour of $x_P F_2^{D(3)}$. The precision data of F_2 makes it possible to see a very significant rise with Q^2 . The $x_P F_2^{D(3)}$ data does not have the precision needed for a clear Q^2 dependence. There is a trend similar to that of F_2 , but given the large errors of the data, the behaviour is also consistent with no Q^2 dependence.

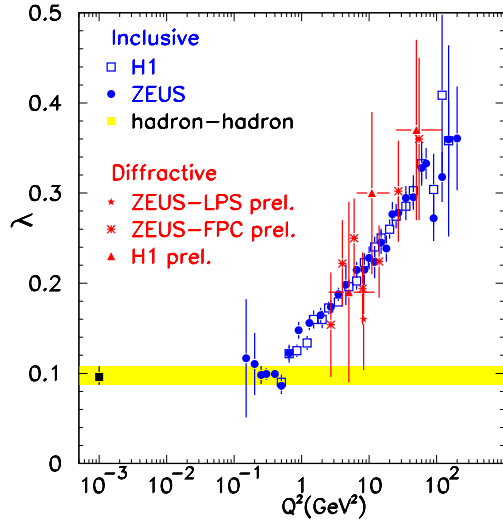


Figure 3. The Q^2 dependence of λ obtained from fits to $F_2 \propto x^{-\lambda}$ and $x_P F_2^{D(3)} \propto x_P^{-\lambda}$. The band indicates the value corresponding to the soft Pomeron.

3.5. NLO QCD fits to $x_P F_2^{D(3)}$

It has been proven [9] that QCD factorization works for diffractive processes at HERA. This allows to use the DGLAP [10] evolution equations to get diffractive parton distribution functions. Given the fact that for describing diffractive processes one needs more variables, t , x_P , β , Q^2 , one would actually like to evolve in β and Q^2 for fixed t and x_P . t is usually hard to measure and one integrates over it. Thus, ideally one would like to evolve for fixed x_P values. The statistics of the presently available data is not sufficient for carrying this out.

Ingelman and Schlein [11] suggested to consider the exchanged Pomeron as a particle having internal structure. Under this assumption, the diffractive process is described as a multistep event: the proton 'radiates' a Pomeron having a fraction x_P of the proton momentum. The virtual photon interacts in a deep inelastic process off the Pomeron, scattering of a parton in the Pomeron carrying a fraction β of the Pomeron momentum. There is thus a flux factor at the proton vertex, dependent only on x_P (t is integrated out), and a Pomeron structure function $F_2^{D(2)}$. This picture assumes Regge factorization, an assumption which has to be checked by the data.

Using the proven QCD factorization together with the assumed Regge factorization, one gets diffractive parton distributions.

3.6. Regge factorization

The assumption of Regge factorization clearly does not hold in the inclusive case. The value of λ is clearly Q^2 dependent. However both the diffractive H1 data and the LPS data can be described by an NLO QCD fit with one fixed value of $\alpha_P(0)$, as shown by Schätzel [7] and by Capua [8] at this meeting. In case of the LPS data, a cut on $x_P < 0.01$ has to be made. For the H1 analysis, one needs to add the Reggeon contribution. The statistics of the LPS data were not sufficient to repeat the fit in different Q^2 bins. The H1 analysis, shows some indication of a rise of λ with Q^2 (see figure 3), though with quite large error bars. The uncertainty comes not only from the statistics but also from the way one needs to isolate the Pomeron contribution from the Pomeron

+ Reggeon fit.

We can conclude that in inclusive diffractive processes, for $x_P < 0.01$, the data can be consistent with Regge factorization. There is a clear need for more precise data.

3.7. Diffractive parton distribution functions

The H1 data, which have a wide kinematical coverage in Q^2 and in β , have been used to extract diffractive parton distributions (dpdfs), shown in figure 4. One sees a dominance of the gluon distri-

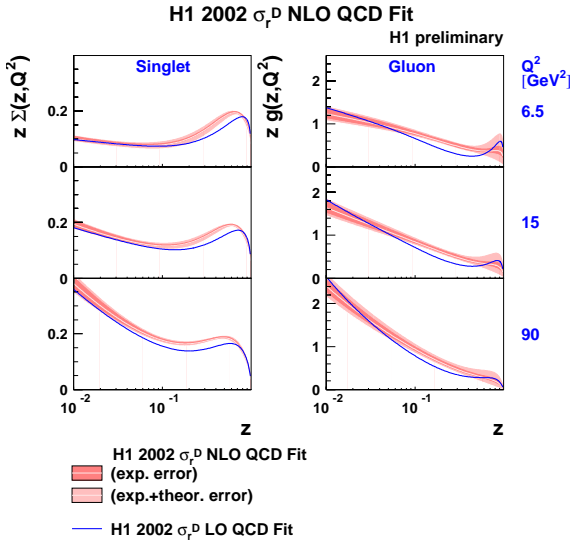


Figure 4. The resulting parton density distributions in the Pomeron, using a NLO QCD fit (shaded line) compared to a LO fit (solid line).

bution, which is the outcome of the fact that the data show positive scaling violation up to quite high β values. This is quantified in figure 5, which shows that for the region $0.01 < \beta < 1$, the gluons carry 80% of the Pomeron momentum. The same conclusion is reached by the LPS analysis. Note that the validity of the diffractive parton distribution functions (dpdfs) is in the following

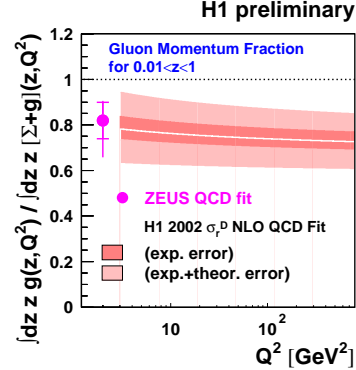


Figure 5. The gluon momentum fraction from a NLO QCD fit, as a function of Q^2 .

kinematic region: $Q^2 > 3 \text{ GeV}^2$, $M_X > 2 \text{ GeV}$ and $x_P < 0.05$. Are these dpdfs portable just like in the inclusive pdfs case? In other words, does QCD factorization work?

3.8. QCD factorization test

The diffractive parton distributions, obtained by H1 from the NLO QCD fit, were used to calculate expectations of other diffractive processes. The agreement with data is very good for diffractive D^* as well as for diffractive dijet production [12]. However, the expectations for the Tevatron results are by one order of magnitude too high [13]. This is not surprising as QCD factorization should not hold for diffractive hadron-hadron reactions. Furthermore, the Tevatron data is measured in the kinematic region $0.035 < \xi < 0.095$, where the Reggeon exchange dominates and thus would not be called diffraction. As mentioned above, the validity of the H1 fit is for $x_P < 0.05$ (x_P at HERA is ξ at the Tevatron). The fact that QCD factorization seems to fail for hadron-hadron data is also explained by introducing the notion of survival probability of the rapidity gap [14]. Taking it at face value, this would mean that for the Tevatron processes, the survival probability is about 0.1. Since the photon has a hadronic part ('resolved photon'), this notion can be tested in diffractive photoproduction of dijets [15,12]. Indeed it seems that using a

survival probability of 0.34 [16], one can describe the resolved photon data. There seems to be some uncertainty about the conclusion concerning the direct part: while the H1 measurement is below the expectations, the ZEUS result is consistent with it.

An interesting attempt to fit the combined data of inclusive and inclusive diffraction data was carried out by Martin, Ryskin and Watt [17], who included absorption correction to the QCD analysis. While the quark distributions they get are not very different from those of H1, their gluon distribution is significantly lower than the H1 one. This results in expectations which are by almost factor of 3 lower than the H1 ones for the comparison with the Tevatron data (see figure 6). In

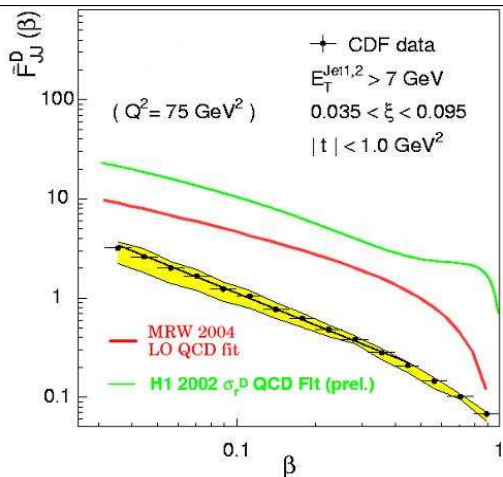


Figure 6. Effective diffractive structure function for dijet production in $p\bar{p}$ interactions as a function of β , compared to expectations of different sets of diffractive parton distribution functions.

this case the survival probability would be closer to that of the resolved photon case.

3.9. Ratio of σ^D to σ_{tot}

Diffractive processes were said to constitute about 10% of the total inclusive DIS processes.

However, the ratio of σ^D/σ^{tot} is Q^2 dependent. It can be as high as 20% at $Q^2 \approx 3 \text{ GeV}^2$, going down to about 10% at $Q^2 \approx 30 \text{ GeV}^2$, as can be seen in fig 7, where this ratio is shown as a function of Q^2 , for the kinematic region $200 < W < 245 \text{ GeV}$, $M_X < 35 \text{ GeV}$, and $M_N < 2.3 \text{ GeV}$. One should however keep in mind

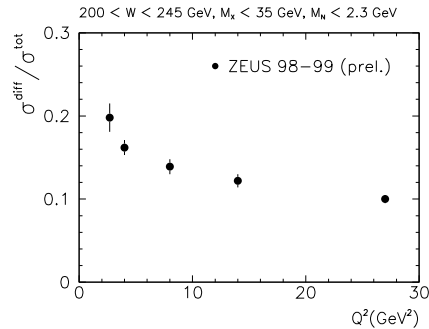


Figure 7. The ratio of diffractive to total cross section as a function of Q^2 , for a selected kinematic region.

that the Q^2 dependence might be an outcome of the fact that in this presentation of the ratio, different regions of β are covered for different values of Q^2 . Note that this ratio at $Q^2 = 100 \text{ GeV}^2$ goes down to $\approx 5\%$ for $x_F < 0.03$ [7].

This ratio has been measured for the first time for Charged Current diffractive processes [7,18]. It is in the range of 2-3 % for x_F and $x < 0.05$.

One can calculate the ratio of diffractive to total cross section for specific processes and check whether the parton distributions obtained from the NLO QCD analysis fulfill the Pumplin bound [19]. This was done in [16] for diffractive to inclusive dijet production induced by gluons and is displayed in figure 8. As seen, the bound is clearly violated for relatively low scales at low x . This might indicate that unitarity effects are already present in the gluon sector.

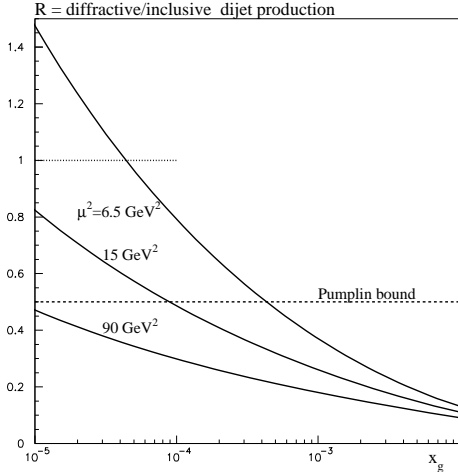


Figure 8. The ratio of diffractive to inclusive dijet production cross section as a function of x of the gluon for different scales of the hard scattering, for the recent H1 diffractive parton distribution functions. Also shown is the unitarity limit, called Pumplin bound.

3.10. Summary on inclusive diffraction

This subsection is more a presentation of some questions than a real summary. Is Regge factorization broken? Also for $x_P < 0.01$? There is a need for more precise measurements to come to a clear conclusion. Ideally, so as not to be dependent on the Regge factorization assumption in diffraction, one would like to do a QCD analysis for fixed values of x_P . This will need much higher statistics than presently available.

There is a breaking of QCD factorization when using the parton distribution densities to compare to hadron-hadron data. This is interpreted by the introduction of the large rapidity gap survival probability. The value of the survival probability seems to be in the range of 0.1-0.3.

The presently obtained gluon momentum densities seem to give results which are violating the Pumplin bound, in certain kinematical regions. This could be the indication of the presence of unitarity effects.

There is a large ratio of diffractive to total cross

section which decreases with Q^2 .

4. Exclusive diffractive processes

4.1. Introduction

This section describes exclusive processes like electroproduction of vector mesons or Deeply Virtual Compton Scattering (DVCS). The situation in these cases is much simpler as these processes are clearly diffractive processes at the high energies where they are measured. There still exist the problem of isolating the 'elastic' process from the proton dissociative one. By measuring the cross section for a limited low t range, the contribution of the latter is minimized.

4.2. Soft to hard transition

One of the nice features seen in these data is the transition from soft to hard processes as one increases the scale. This transition is seen also

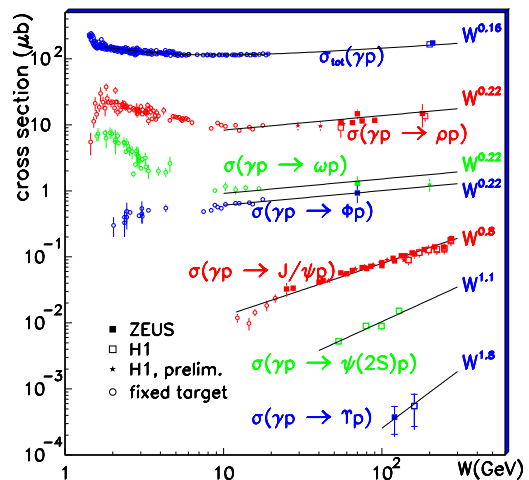


Figure 9. A compilation of elastic photoproduction of vector mesons, as a function of W . The total γp cross section is plotted for comparison.

for the photoproduction of vector mesons, where the mass serves as the scale. Figure 9 shows the

photoproduction cross section as a function of the γp center of mass energy, W , for different vector mesons. The light vector mesons, ρ , ω and Φ show an energy dependence which is characteristic of a soft process (the total γp cross section is also shown for comparison). For the heavier vector mesons, the energy dependence becomes much steeper, as expected from hard processes. Note also that the real part of the amplitude increases with the hardness of the process and is a further reason for the sharp energy dependence.

The soft to hard transition can also be seen for a given vector meson, by changing the Q^2 of the process. The cross section is parameterized as W^δ and δ is seen to increase with Q^2 . To compare all the vector mesons on one plot [20] one shows δ as function of $Q^2 + M_V^2$, with M_V being the mass of the vector meson. As seen in figure 10, one gets an increase of δ from values of about 0.2 (soft) at the low scale end to a value of about 1 (hard) at high scales.

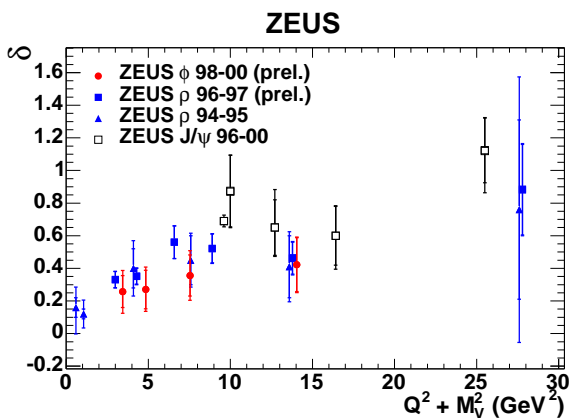


Figure 10. The parameter δ from a fit of the form W^δ to the cross section data of exclusive production of VMs, as a function of $Q^2 + M_V^2$.

4.3. Effective Pomeron trajectory

Using the energy dependence of vector meson electroproduction at fixed t values, one can obtain the parameters of the effective trajectory ex-

changed in the process. This way the effective trajectory of the Pomeron was determined for the ρ , ϕ and J/ψ electroproduction. A summary plot of the intercepts and slopes for all three VMs, as function of $Q^2 + M_V^2$, is presented in figure 11. The intercept of the low mass VMs are consistent

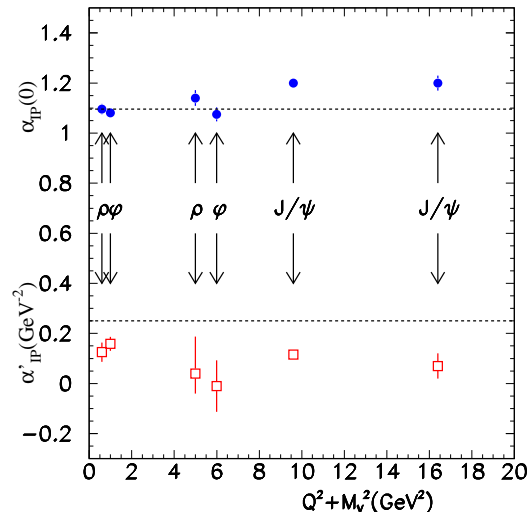


Figure 11. Compilation of $\alpha_P(0)$ and α'_P values, extracted in exclusive VM production, as a function of $Q^2 + M_V^2$.

with that of the soft Pomeron. This is not the case for the J/ψ which has a significantly higher intercept. As for the slope, all values are lower than that of the soft Pomeron, as expected from hard processes.

4.4. Sizes of vector mesons

The t distribution of the VMs can be well described by an exponentially falling cross section, with a slope b . This slope is connected to the size of the VM. At low Q^2 the size of the light VMs is large, decreasing with Q^2 from a value of ≈ 10 GeV^{-2} to about 5 GeV^{-2} . For the J/ψ the size is small already at low Q^2 . This can be seen in

figure 12, where the slope b is plotted as function of Q^2 . The dotted lines are just to guide the eye.

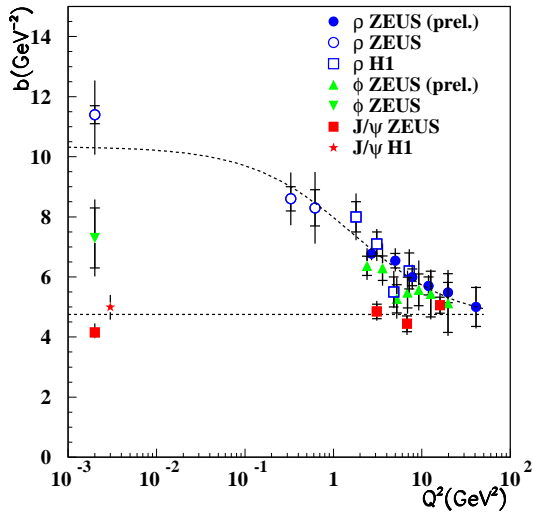


Figure 12. Exponential slope of the t distribution measured for exclusive VM production as a function of Q^2 . The lines are to guide the eye.

The data seem to converge at high Q^2 on a value of $b \approx 5 \text{ GeV}^{-2}$.

4.5. $R = \sigma_L/\sigma_T$

The ratio R of the longitudinal photon cross section, σ_L , to that of the transverse photon, σ_T , can be obtained by studying the decay distribution of the VM and assuming s-channel helicity conservation. This has been done for ρ [21,22,20], ϕ [20] and J/ψ [20]. Figure 13 shows as an example the very impressive preliminary measurements of R as a function of Q^2 for the ρ VM by the COMPASS collaboration [21]. For all VMs, R is rising with Q^2 . A compilation of R for all three VMs is shown in figure 14, as function of Q^2 . The lines are a fit to the data of the form $R = a(Q^2/M_V^2)^b$, which indicate that R scales with Q^2/M_V^2 .

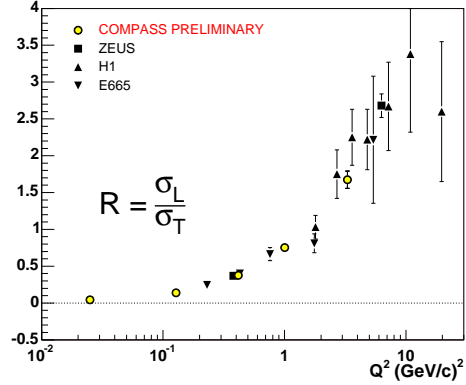


Figure 13. The Q^2 dependence of R for exclusive ρ^0 electroproduction.

4.6. Configurations of the photon

The photon is described as fluctuating into a $q\bar{q}$ pair. When the relative k_T between the pair is small we speak of a large spatial configuration, while if the relative k_T is large, the photon fluctuates into a small spatial configuration. Longitudinal photons have small configurations, while transverse photons consist of both large and small configuration. A small spatial configuration leads to hard processes and thus to a steep energy dependence of the cross section. A large configuration has a shallower energy dependence, as expected in soft processes.

It came therefore as a surprise that the ratio R for the ρ electroproduction process is W independent for W values up to 120 GeV and Q^2 up to 19 GeV^2 [23]. The ratio R is W independent also for J/ψ [20].

This means that for some reason in case of VM electroproduction the large configurations of the transverse photon are suppressed.

Another process which seems to send the same message is DVCS. The energy dependence of this reaction indicates a hard process. The W^δ dependence yields [24] $\delta=0.98\pm 0.44$ for the H1 measurement and $\delta=0.75\pm 0.15^{+0.08}_{-0.06}$ for ZEUS. Such a steep energy dependence would be expected from a dominant longitudinal photon. However, in DVCS one goes from a virtual photon to a

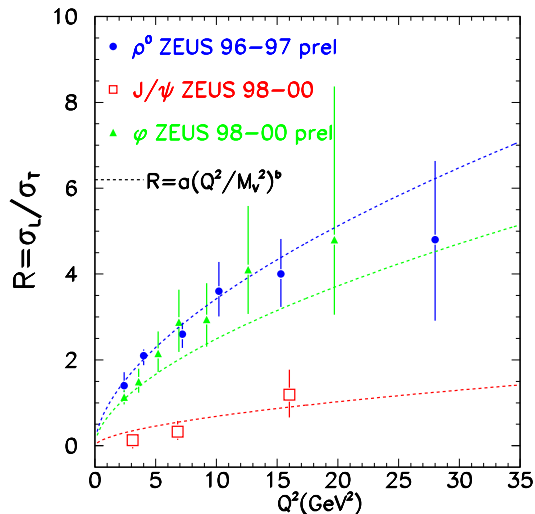


Figure 14. A compilation of the values of R for ρ^0 , ϕ and J/ψ , as a function of Q^2 . The lines are a fit to the data of the form $R = a(Q^2/M_V^2)^b$.

real one, $\gamma^* \rightarrow \gamma$. Assuming s-channel helicity conservation, this means that, since the real photon is transverse, also the initial virtual photon has to be transverse. Thus, the steep energy dependence of the DVCS cross section means that the large configuration in the transverse photon is suppressed.

4.7. Summary on exclusive diffraction

Exclusive diffractive processes become hard once the scale gets large. The properties of the effective Pomeron exchange at the larger scales are consistent with that of a hard process. The large configurations of the transverse photon seem to be suppressed in exclusive VM, including real photon, production.

4.8. Outlook

Diffractive processes are expected to be measured with improved machines and detectors at HERA, the Tevatron and at RHIC. Whether we want it or not, a large portion of the interactions measured at LHC will be of diffractive nature [25].

In fact, the exclusive diffractive production of the Higgs boson has been proposed as a potential background free method to search for the light Higgs at LHC. One can also dream about a future ep collider which will allow to reach kinematic region where phase transitions can be observed. Clearly diffraction is a subject which will occupy us for quite some time to come.

Acknowledgments

It is a pleasure to acknowledge and thank the organizers for the excellent organization of a very pleasant conference in a most beautiful location.

REFERENCES

1. James D. Bjorken, *Hard diffraction and deep inelastic scattering*, Proceedings of DIS94, Eilat, Israel, (ed. A. Levy) p.151, 1994.
2. ZEUS Collab., S. Chekanov et al., DESY-04-131, hep-ex/0408009 (2004).
3. H1 Collab., C. Adloff et al., Nucl. Phys. **B619**, 3 (2001).
4. ZEUS Collab., J. Breitweg et al., Eur. Phys. J. **C6**, 43 (1999).
5. See eg K. Goulianos, *Hadronic diffraction: where do we stand?*, hep-ph/0407035 (2004).
6. K. Golec-Biernat, J. Kwiecinski and A. Szczurek, Phys. Rev. **D56**, 3955 (1997).
7. S. Schätzel (for the H1 Collaboration), *H1 diffractive structure function measurements and QCD fits*, these proceedings.
8. M. Capua (for the ZEUS Collaboration), *ZEUS results on inclusive diffraction*, these proceedings.
9. J.C. Collins, Phys. Rev. **D 557**, 3051 (1998); erratum Phys. Rev. **D 61**, 2000 (1998); A. Berera and D.E. Soper, Phys. Rev. **D 53**, 6162 (1996); L. Trentadue and G. Veneziano, Phys. Lett. **B 323**, 201 (1994).
10. Y.L. Dokshitzer, Sov. Phys. JETP **46**, 641 (1977) [Zh. Eksp. Teor. Fiz. **73**, 1216 (1977)]; V.N. Gribov and L.N. Lipatov, Yad. Fiz. **15**, 1218 (1972) [Sov. J. Nucl. Phys. **15**, 675 (1972)]; V.N. Gribov and L.N. Lipatov, Yad. Fiz. **15**, 781 (1972) [Sov. J. Nucl. Phys. **15**,

- 438 (1972)]; G. Altarelli and G. Parisi, Nucl. Phys. **B 126**, 298 (1977).
11. G. Ingelman and P.E. Schlein, Phys. Lett. **B 152**, 256 (1985).
 12. S. Vinokurova (for the H1 Collaboration), *The diffractive production of charm and jets*, these proceedings.
 13. C. Mesropian (for the CDF Collaboration), *Diffractive production at CDF in run II*, these proceedings.
 14. See eg E. Gotsman, E. Levin and U. Maor, Phys. Lett. **B 438**, 229 (1998).
 15. R. Renner (for the ZEUS Collaboration), *ZEUS results on diffractive dijets*, these proceedings.
 16. A.B. Kaidalov et al., Phys. Lett. **B 567**, 61 (2003).
 17. A.D. Martin, M.G. Ryskin and G. Watt, Phys. Rev. **D 70**, 091502 (2004).
 18. J. Rautenberg (for the ZEUS Collaboration), *Diffractive charged current (ZEUS)*, these proceedings.
 19. J. Pumplin, Phys. Rev. **D 8**, 2899 (1973).
 20. R. Ciecielski (for the ZEUS Collaboration), *Recent ZEUS results on vector mesons*, these proceedings.
 21. A. Sandacz (for the COMPASS Collaboration), *Diffractive ρ^0 production at COMPASS*, these proceedings.
 22. O. Grebenyuk (for the HERMES Collaboration), *Exclusive electroproduction of pions and vector meson at HERMES*, these proceedings.
 23. See eg H. Abramowicz, *Diffractive scattering*, hep-ex/0410002 (2004).
 24. K. Hiller (for the H1 Collaboration), *High $|t|$ diffraction and DVCS from H1*, these proceedings.
 25. S. White, these proceedings.

ZEUS

